X-Ray Spectral Imaging of Puppis A with Suzaku

Una Hwang,[1,2] Robert Petre[2] and Kathryn A. Flanagan[3]

[1] *The Johns Hopkins University, Baltimore, MD, USA*
[2] *NASA Goddard Space Flight Center, Greenbelt, MD, USA*
[3] *MIT, Cambridge, MA, USA*

We report the detection of X-ray emitting ejecta in the middle-aged Galactic supernova remnant Puppis A from an imaging and spectral survey with the Suzaku Observatory. Energy-selected images from five observations covering the eastern and middle portions of the remnant reveal a region inside the northern apex that is very highly enriched in Si. Regions with lesser enhancements of other elements such as O, Ne, and Mg are also seen, and confirmed by the spectra. The location of the large Si clump is radially outside that of X-ray emitting O ejecta relative to the expansion center, indicating that the explosively synthesized Si ejecta were mixed with and propelled beyond hydrostatically synthesized O ejecta. There appears to be little spatial correlation between the compact ejecta knots seen in O emission in the optical and the large-scale ejecta enhancements seen in X-rays by Suzaku.

§1. Introduction

Puppis A is a middle-aged ($\sim$ 4000 year old) Galactic remnant in which oxygen ejecta have been observed optically (Winkler & Kirshner 1985) and is suggested in X-rays (Canizares & Winkler 1981, Hwang et al. 2005). Its core-collapse origin is firmly established by the presence of an X-ray emitting neutron star associated with the remnant (Petre et al. 1996, Winkler & Petre 2007).

We present a partial X-ray survey with the Suzaku X-ray Imaging Spectrometer covering the eastern and central portions of Puppis A. The motivation was to search for X-ray emission corresponding to the oxygen ejecta.

§2. Observations

Five fields were observed with Suzaku at the beginning of the AO-1 phase in 2006 (ObsID 501086010, 501087010, 501088010, 501089010, 50109000). The observations were optimized to detect and map the O VII Resonance line at 574 eV and O VIII Lyα at 654 eV. Given the high overall count rates in three of the five fields, the front-side XIS detectors were operated in 4s burst mode for those observations.

Mosaicked images were produced for all the major spectral features, including O VII He-like blend (including the resonance line), O VIII Lyα, Fe L (primarily Fe XVII at 827 eV), and the He-like blends of Ne, Mg, and Si. The broadband mosaic is shown in Fig. 1, with the ROSAT HRI contours overlaid.

We also made difference images of the lines relative to the broadband emission to highlight areas of relatively stronger or weaker line emission, ratio images of two line images (with the underlying continuum included) to diagnose plasma conditions, and ratio images of the continuum-subtracted line emission relative to continuum to look for ejecta enhancements ("equivalent width" or EQW; here the underlying continuum

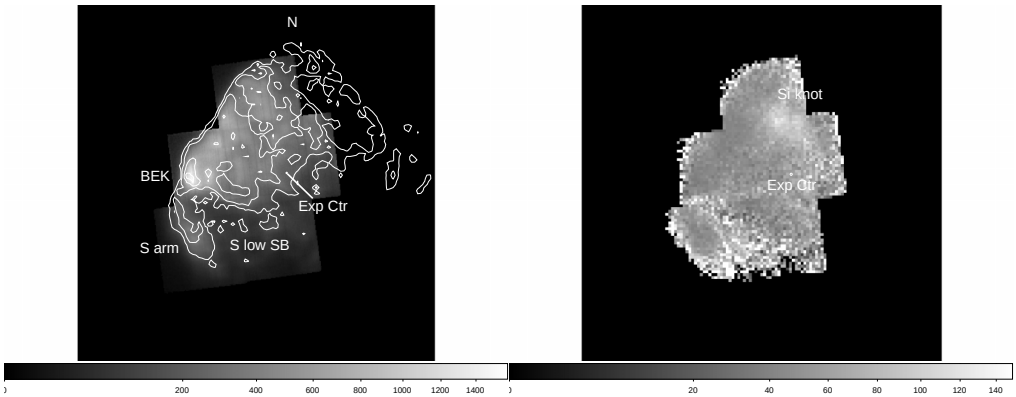

Fig. 1. (left) Broadband mosaic of the Suzaku XIS observations of Puppis A with contours from the ROSAT High Resolution Imager (HRI) overlaid. Some features discussed in the text are labelled. (right) Line-to-continuum "equivalent width" image of Si XIII. The explosion center determined by Winkler & Kirshner (1985) is indicated in both panels.

is extrapolated from a nearby line-free region). As spectral differences can arise from any combination of a number of factors, including absorption, temperature, ionization, and element abundance, we follow up the imaging analysis by fitting selected spectra to ascertain the cause of the spectral differences. For this purpose we used the response matrices and effective area files released on 2006 Feb. 13 and 2006 April 15, respectively.

§3. Results

The brightest feature in all the images is the Bright Eastern Knot (BEK), which is located at the indentation of the eastern X-ray shock front (see Fig. 1). The outside part of this feature is seen to be very soft, as is already known from Chandra observations of this region (Hwang et al. 2005), based on its relatively higher brightness in the lowest energy line images. Farther to the north, the straight edge of the northeast shock front is at higher temperature, and produces relatively more emission from higher excitation lines.

Some examples of the spatial variations in the line emission are illustrated by the difference images in Fig. 2. O emission is relatively prominent at the eastern edge of the BEK, but deficient along the northeastern shock front. There are also two relatively compact "knots" of O in the interior regions of the remnant, the stronger one being to the west. The Fe L emission, which is mostly Fe XVII at 827 eV, appears to be most enhanced in the region of the BEK and along the southeastern arm (S arm, see Fig. 1). Mg (and also Si which is not shown) has preferentially more emission along the shock front than other line images. A prominent enhancement is seen for Si inside the northern apex of the remnant.

The Si knot is most strikingly seen in the Si EQW image (right panel of Fig. 1). While the fitted absolute element abundances tend to be subsolar throughout Puppis A in our nonequilibrium ionization models (NEI and pshock in XSPEC), comparison

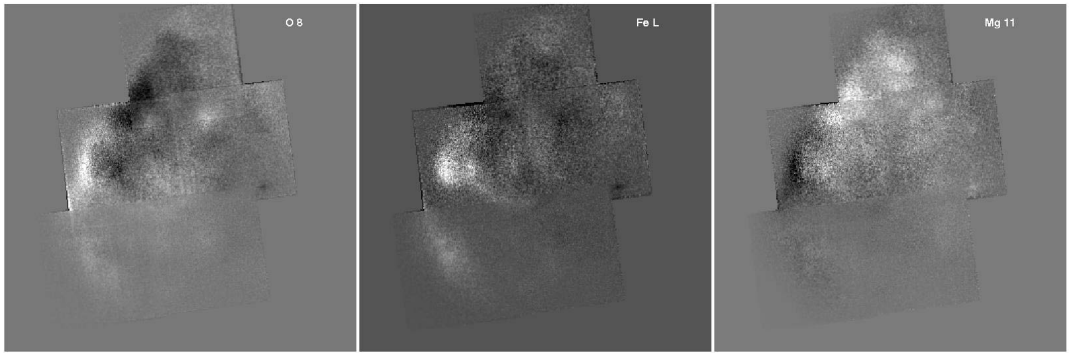

Fig. 2. Differences images of the energy-selected line images of O VIII, Fe L (mostly Fe XVII at 827 eV), and Mg XI relative to the broadband image. White denotes an excess and black a deficit relative to the broadband image.

of the spectra from this region with those from the northeast shock front where Si line emission is prominent but Si EQW is low, confirms that the abundances of Si are relatively enhanced at the knot. The fitted Si abundance of the knot is 1.0 ± 0.05 relative to the solar value, compared to 0.21 (+0.03, −0.01) at the shock front. The column densities and temperatures of the two regions are similar, at roughly $N_H = 4 \times 10^{21}$ cm^{-2} and kT = 0.70–0.80 keV; the ionization age at the knot is lower at $n_e t = 8.0(+0.2, -0.3) \times 10^{10}$ cm^{-3} s than at the shock front, where it is $2.9 \pm 0.2 \times 10^{11}$ cm^{-3} s. Both spectra are shown in the top panels of Fig. 3.

Enhancements in other element abundances are more modest. At the brighter

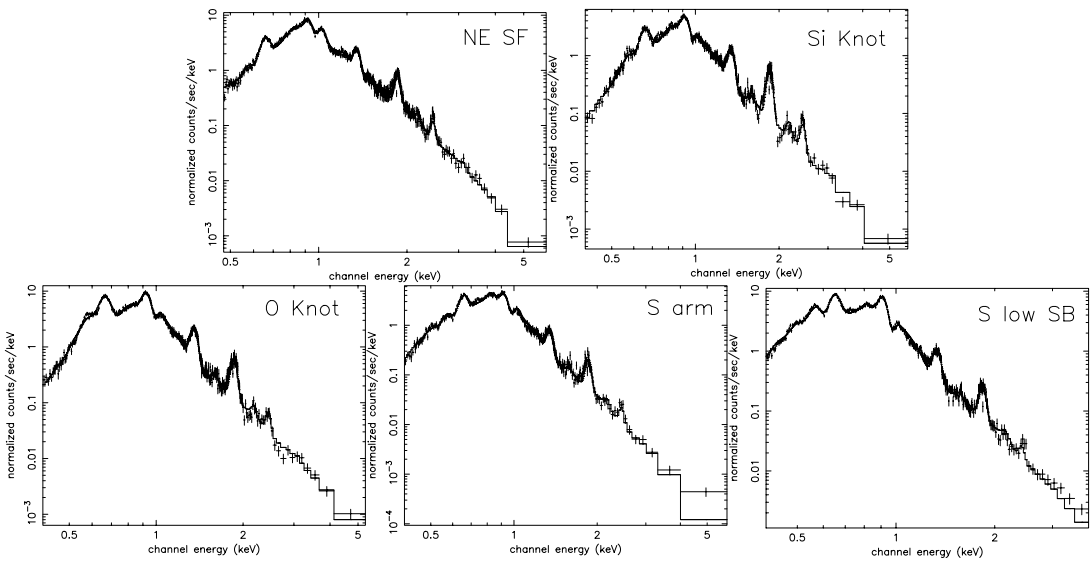

Fig. 3. (top) Spectra from the NE shock front and the Si knot. Both show strong Si line emission near 1.8 keV, but the fitted Si abundance is four times higher at the knot. (bottom) Spectrum of an O-enriched knot, and of regions on the S arm and in the S low surface brightness region where O VII/O VIII is enhanced. The O lines are at 574 (resonance) and 654 eV (Ly α).

(westernmost) of the two O knots seen in Fig. 2, spectral fits confirm that the O abundances for the knots are enhanced by a factor of two over typical values elsewhere in the remnant. The spectrum for this O knot is shown in the bottom left panel of Figure 3.

Aside from element abundance enhancements, the ratio images of two lines of the same element help to diagnose plasma conditions. The line ratio images of O VII/O VIII and Ne IX/Ne X both show enhancements in the southern low surface brightness region (S low SB, see Fig. 1). Comparison of spectra in the S low SB region and in the adjacent S arm region shows that the relative enhancement of the He-like line emission in the S low SB region is primarily due to a lower ionization age. The two spectra shown in Fig. 3 have nearly the same absorption column, temperature, and abundances, but that of the S arm has a higher ionization age of $n_e t = 2.1 \pm 0.1 \times 10^{11}$ cm^{-3} s compared to the S low SB region where it is $8.6(+0.3, -0.05) \times 10^{10}$ cm^{-3} s. The difference in ionization age is enough to affect the relative population of the He- and H-like ions and their line strengths, so that the He-like lines are relatively stronger in the S low SB region.

§4. Discussion

The position of the Si-enhanced knot is just outside that of the O-enhanced knot, nearly in a line with the expansion center determined for the optically emitting O knots by Winkler & Kirsher (1985). Since the O should have been produced hydrostatically by the progenitor well before the explosion, whereas the Si was produced explosively during the supernova event, we expect the Si to have been initially located *interior* to the O rather than outside as is now observed. The observed arrangement indicates that the Si were propelled beyond the O ejecta during the explosion in a manner reminiscent of the Si and Fe overturns observed in the much younger 300-year old Cassiopeia A supernova remnant (Hughes et al. 2000). In Cas A, however, both ejecta species involved are explosive products.

There is little correlation between the optically and X-ray emitting ejecta in Puppis A. The position of the O knot does not overlap that of the optically emitting ejecta knots, which are located eastward, and there is no obvious evidence of enhancement of O in the X-ray emitting gas at the optical knots. This is in contrast to Cas A, where the optical and X-ray emitting ejecta track each other well.

We are grateful to H. Mori for expert help in configuring the observation. We also note that the Si ejecta results were discovered nearly simultaneously by T. Satoru et al. using XMM-Newton (paper in preparation).

References

1) C. R. Canizares and P. F. Winkler, Astrophys. J. **246** (1981), L33.
2) J. P. Hughes et al., Astrophys. J. **528** (2000), L109.
3) U. Hwang, K. A. Flanagan and R. Petre, Astrophys. J. **635** (2005), 355.
4) R. Petre, C. M. Becker and P. F. Winkler, Astrophys. J. **465** (1996), L43.
5) P. F. Winkler and R. P. Kirshner, Astrophys. J. **299** (1985), 981.
6) P. F. Winkler and R. Petre, Astrophys. J. (2007), submitted.